Sol-gel synthesis and characterization of the photocatalyst $BaCo_{1/3}Nb_{2/3}O_3$

JIANG YIN
Precursory Research for Embryonic Science and Technology, Japan Science and Technology Agency (JST), Japan; Ecomaterials Center, National Institute for Materials Science (NIMS), 1-2-1 Sengen, Tsukuba, Ibaraki 305-0047, Japan

ZHIGANG ZOU
Ecomaterials and Renewable Energy Research Center, Nanjing University, Nanjing, 210093, China

JINHUA YE*
Precursory Research for Embryonic Science and Technology, Japan Science and Technology Agency (JST), Japan; Ecomaterials Center, National Institute for Materials Science (NIMS), 1-2-1 Sengen, Tsukuba, Ibaraki 305-0047, Japan

Published online: 4 February 2006

The photocatalyst $BaCo_{1/3}Nb_{2/3}O_3$ has been synthesized at 750°C by using a sol-gel process, and the surface area is 19.70 m^2/g. While the surface area of the powder synthesized by using a solid state reaction process is 2.2 m^2/g. It was characterized by X-ray diffraction, scanning electron microscopy(SEM), UV-vis diffuse reflectance spectroscopy, Raman scattering spectroscopy and the measurement of the photocatalytic activity in evolving H_2 from CH_3OH/H_2O solution with the Pt co-catalyst under visible light irradiation. From the SEM image, $BaCo_{1/3}Nb_{2/3}O_3$ powder calcined at 750°C is dispersive, and the average particle size is about 30 nm. Raman scattering spectrum at room temperature shows that, due to the different ionic radius of the Co^{2+} and Nb^{5+} ions, $BaCo_{1/3}Nb_{2/3}O_3$ may has a distorted perovskite structure. Under visible light irradiation ($\lambda > 420$ nm), the formation rate of H_2 evolution from CH_3OH/H_2O solution with the 0.5 wt% Pt co-catalyst is about 18.1 μmol/h·gcat. for the photocatalyst $BaCo_{1/3}Nb_{2/3}O_3$, much higher than that of $BaCo_{1/3}Nb_{2/3}O_3$ powder synthesized by the solid state reaction process.

1. Introduction

In the past three decades, extensive efforts have been made to develop semiconductor photocatalysts, which can split water and decompose environmental contaminants under UV or visible light irradiation [1–3]. Many materials have been found to show high photocatalytic activity under UV light irradiation [4–6]. While in the view of solar energy conversion, the photocatalyst active under visible light irradiation is more favorable. Generally, it is believed that the valence band of the transition metal oxides with an empty d orbital is composed of the O 2p level, and the conduction band is composed of the d level [7]. As known, the conduction band (Ti 3d) of TiO_2(E_g−3.0 eV) is just above the potential of the H^+/H_2 electrode, and the valence band (O 2p) is more than 1.0 eV below the potential of the O_2/H_2O electrode [8]. In case of $Sr_2Nb_2O_7$, the conduction band(the Nb 4d level) is about 0.8 eV above the potential of the H^+/H_2 electrode, and the valence band(O 2p) is about 1.8 eV below the potential of the O_2/H_2O electrode [9]. So it is suggested to introduce a new valence band instead of the O 2p orbital or introduce a new conduction band instead of the empty d orbital for developing new transition-metal oxide photocatalysts, responding to visible light irradiation. Recently, $TiO_{2-x}N_x$ has been reported to respond to visible light irradiation due to the introduction of a new valence band(the N 2p level) [2]. In our previous work [10], the photocatalyst $BaCo_{1/3}Nb_{2/3}O_3$ with unique crystal and electronic structure was prepared by a solid state reaction process. It shows favorable photocatalytic activity under visible light irradiation ($\lambda > 420$ nm), where it was suggested that the split t_{2g} or e_g orbital under the crystal field of

*Author to whom all correspondence should be addressed.
0022-2461
DOI: 10.1007/s10853-005-3651-7

the octahedron acts as the valence band instead of the O 2p level. For improving the photocatalytic activity, in this work, $BaCo_{1/3}Nb_{2/3}O_3$ powder was synthesized by a sol-gel process, and its photocatalytic activity under visible light irradiation(λ>420 nm) was also investigated.

2. Experimental section

$BaCo_{1/3}Nb_{2/3}O_3$ polycrystalline powder was synthesized by a sol-gel process. Here, $Ba(HCOO)_2$, $(CH_3COO)_2Co{\cdot}4H_2O$, and $Nb(OC_2H_5)_5$ were used as precursors. The flow chart of the synthesis was shown in Fig. 1. In the experiment 7.0 g $BaCo_{1/3}Nb_{2/3}O_3$ was synthesized. According to the chemical stoichiometry, the amount of the pure starting materials for $Ba(HCOO)_2$, $(CH_3COO)_2Co{\cdot}4H_2O$ and $Nb(OC_2H_5)_5$ are 6.699, 2.177 and 5.564 g, respectively. $Ba(HCOO)_2$ was dissolved in the mixed solution of 40 ml CH_3OH and 20 ml CH_3COOH at 80°C, and $(CH_3COO)_2Co{\cdot}4H_2O$ was dissolved in the mixed solution of 20 ml CH_3OH and 10 ml CH_3COOH at 80°C. These solutions were continuously stirred by using a magnetic stirrer during the dissolution. The red transparent solution of $(CH_3COO)_2Co$ was dropped slowly to the transparent solution of $Ba(HCOO)_2$ with a burette. The mixed solution was transparent. Then $Nb(OC_2H_5)_5/CH_3OH$ solution, as prepared in a glove box purged with argon atmosphere to prevent the chemical reactions with moisture and air, was dropped slowly to the mixed solution of $Ba(HCOO)_2$ and $(CH_3COO)_2Co$. As shown in Fig. 1, the solvent of the mixed solution was removed at 500°C for 4 h in an alumina crucible. Thus the amorphous gloomy black powder was obtained. Finally, the amorphous powder was calcined at 650–850°C for 2 h.

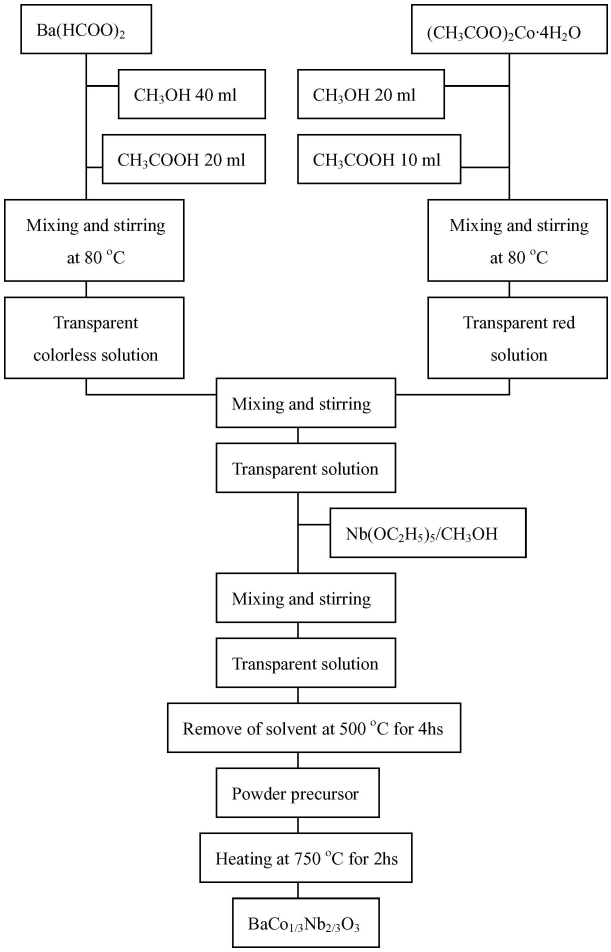

Figure 1 The flow chart of the synthesis for the photocatalyst $BaCo_{1/3}Nb_{2/3}O_3$ by the sol-gel process.

The crystal structure of $BaCo_{1/3}Nb_{2/3}O_3$ powder was checked by using X-ray diffraction (JEOL JDX-3500, Tokyo Japan), and the morphology of the powder sample was investigated by using SEM (JEOL JSM-6500, Tokyo, Japan). The surface area of $BaCo_{1/3}Nb_{2/3}O_3$ powder was determined by the BET measurement. Raman scattering spectrum of $BaCo_{1/3}Nb_{2/3}O_3$ powder was investigated by a laser Raman spectrophotometer(Jasco NRS-1000) at room temperature. The power of the incident laser beam was 100 mW with monochromatic wavelength 532 nm.

The photocatalytic reaction was performed by using a closed gas circulation system, as described in [10]. The H_2 evolution was performed in CH_3OH/H_2O solution with the Pt co-catalyst. The precursor for the Pt co-catalyst is H_2PtCl_6. The photocatalyst powder was added to the Pt co-catalyst solution. The slurry was put in a supersonic oscillator for 20 min, and then left in a baker, until all the water evaporated. The powder as obtained was heated at 500°C for 2 h in air.

3. Results and discussion

3.1. Physical characterization

Fig. 2 shows X-ray diffraction patterns of $BaCo_{1/3}Nb_{2/3}O_3$ powders calcined at different temperatures. It is obvious that after calcined at 650°C,

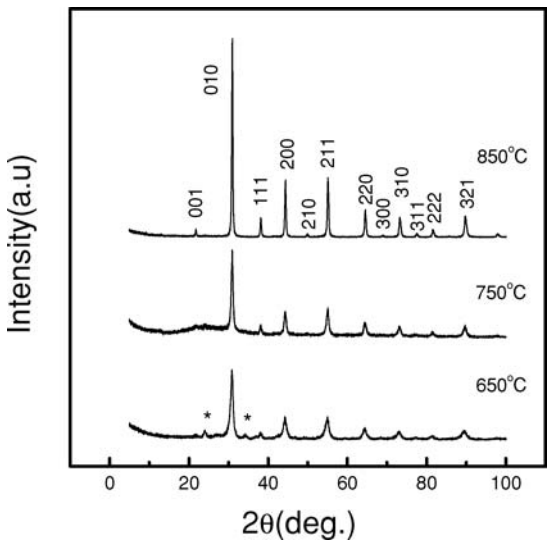

Figure 2 X-ray diffraction patterns of $BaCo_{1/3}Nb_{2/3}O_3$ powder calcined at different temperatures.

$BaCo_{1/3}Nb_{2/3}O_3$ becomes the main phase in powder, although there are some impurity phases, as indicated by the asterisk in Fig. 2. At 750°C, the powder was well crystallized with $BaCo_{1/3}Nb_{2/3}O_3$ phase. When calcined at 850°C, the corresponding intensity of the diffraction peaks for $BaCo_{1/3}Nb_{2/3}O_3$ powder becomes stronger, indicating an improvement of the crystallinity for $BaCo_{1/3}Nb_{2/3}O_3$. It is also obvious that with the increase of the calcination temperature, the full width of half-maximum (FWHM) for $BaCo_{1/3}Nb_{2/3}O_3$ powder becomes smaller. It means that the higher calcination temperature results in the larger particle size. All the diffraction peaks can be indexed according to a cubic perovskite phase. The surface area of $BaCo_{1/3}Nb_{2/3}O_3$ powder calcined at 750°C, as measured by the BET measurement, is 19.7 m^2/g, and that of the powder prepared by the solid state reaction process is 2.2 m^2/g. The morphology and crystallinity of $BaCo_{1/3}Nb_{2/3}O_3$ powders were investigated by using SEM. Fig. 3a shows the SEM morphology of $BaCo_{1/3}Nb_{2/3}O_3$ powder synthesized by solid state reaction method. $BaCo_{1/3}Nb_{2/3}O_3$ particles distribute aggregatively, and the average particle size is about 200 nm. Fig. 3b shows the SEM morphology of $BaCo_{1/3}Nb_{2/3}O_3$ powder synthesized by the sol-gel process calcined at 750°C. $BaCo_{1/3}Nb_{2/3}O_3$ particles distribute dispersively and uniformly, and the average particle size is about 30 nm.

Raman scattering spectrum and the infrared(IR) reflection spectrum have been used to investigate the lattice dynamics of ABO_3 perovskite widely [11–13]. In a ABO_3 perovskite with non-cubic symmetry, the lattice vibration modes are assigned to three main branches: (a) the stretching branch, in which, the B-O bond distance is modulated; (b) the bending branch, in which, the B–O–B bond angle is modulated; (c) the external branch, in which, atom A translates with respect to BO_6 octahedron. The Raman scattering spectrum of $BaCo_{1/3}Nb_{2/3}O_3$ powder as calcined at 850°C at room temperature is shown in Fig. 4. Eight phonon modes at about 100.0 cm^{-1}, 143.9 cm^{-1}, 170.3 cm^{-1}, 286.7 cm^{-1}, 370.3 cm^{-1}, 422.5 cm^{-1}, 519.3 cm^{-1} and 767.3 cm^{-1} could be found clearly for $BaCo_{1/3}Nb_{2/3}O_3$.

Although the complete assignment is not possible because a polarization analysis is not available, according to the method adopted by Perry *et al*. [14] in the IR study of perovskite, from low to high frequency the Raman spectrum of $BaCo_{1/3}Nb_{2/3}O_3$ can be interpreted as composed of three main phonon branches. The first mode at 100.0 cm^{-1} should be ascribed to the external mode, and the branch around 370.3 cm^{-1}, consisting of six components, is ascribed to the bending branch, while the mode at 767.3 cm^{-1} should be ascribed to the stretching mode.

As known, no Raman active mode can be obtained for ABO_3 perovskite with the cubic symmetry. Although it was reported that $BaCo_{1/3}Nb_{2/3}O_3$ shows a cubic perovskite structure [15], from Fig. 4 the triple-cubic perovskite structure, just like $BaIn_{1/2}Nb_{1/2}O_3$ [16], is more

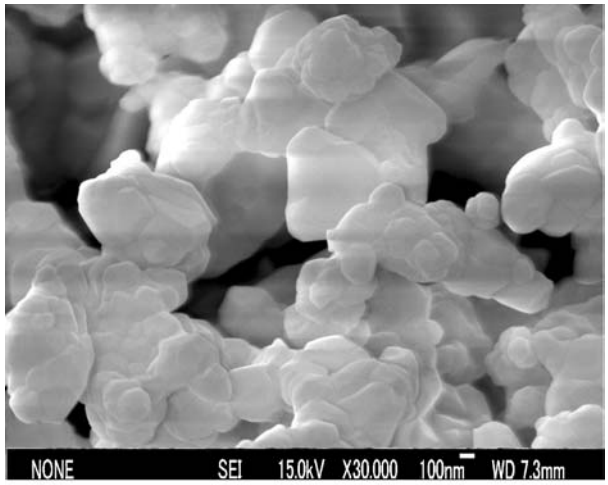

Figure 3 SEM images of $BaCo_{1/3}Nb_{2/3}O_3$ powder as synthesized by (a) solid state reaction process, and (b) sol-gel process calcined at 750°C.

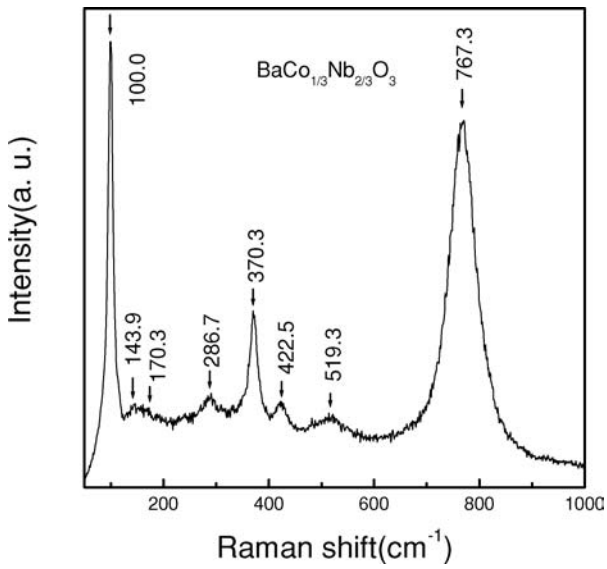

Figure 4 Room temperature Raman scattering spectrum of $BaCo_{1/3}Nb_{2/3}O_3$ powder as calcined at 850°C.

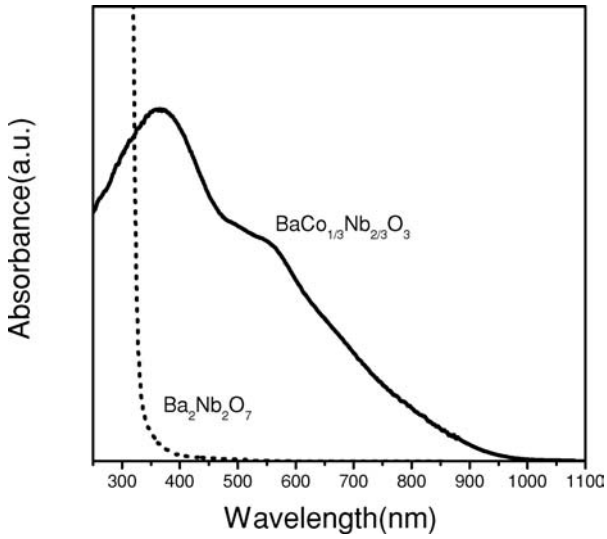

Figure 5 UV-vis diffuse reflectance spectrum of $BaCo_{1/3}Nb_{2/3}O_3$ powder calcined at 750°C.

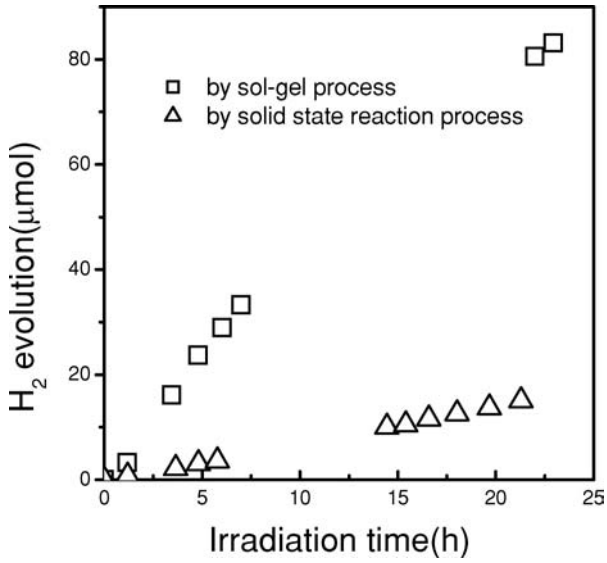

Figure 6 The formation rate of H_2 evolution from CH_3OH/H_2O solution with the Pt co-catalyst under visible light irradiation for the photocatalyst $BaCo_{1/3}Nb_{2/3}O_3$ synthesized by the sol-gel process calcined at 750°C and solid state reaction process (cat.: 0.2 g, co-cat.: 0.5 wt% Pt, CH_3OH: 50 ml, H_2O: 220 ml, Xe lamp, 300 W, $\lambda > 420$ nm).

reasonable for $BaCo_{1/3}Nb_{2/3}O_3$. The observed Raman active vibration modes of $BaCo_{1/3}Nb_{2/3}O_3$ should be ascribed to the lowered symmetry resulted from the local distortion of octahedron due to the different ionic radii of the Co^{2+} and Nb^{5+} ions.

Fig. 5 shows UV-vis diffuse reflectance spectrum of $BaCo_{1/3}Nb_{2/3}O_3$ powder calcined at 750°C. For making a comparison, the UV-vis diffuse reflectance spectrum of the parent phase $Ba_2Nb_2O_7$ is also shown in Fig. 5. The parent phase $Ba_2Nb_2O_7$ only absorbs UV light photons, and the absorption edge is at about 325.4 nm, corresponding to a band gap 3.81 eV. With the unique crystal and electronic structure, $BaCo_{1/3}Nb_{2/3}O_3$ strongly absorbs the visible light photons. It was suggested that the optical absorption of visible light photons corresponds to the electronic excitations from the split Co 3d t_{2g} or e_g states to the Nb 4d states [10].

3.2. Photocatalytic activity

In the experiments, easily reducing reagent CH_3OH was employed to evaluate the photocatalytic activity of the photocatalyst $BaCo_{1/3}Nb_{2/3}O_3$, as synthesized at 750°C. Fig. 6 shows the formation rate of H_2 evolution from CH_3OH/H_2O solution with the Pt co-catalyst under visible light irradiation for the photocatalyst $BaCo_{1/3}Nb_{2/3}O_3$ prepared by the sol-gel process calcined at 750°C and the solid state reaction process (cat.: 0.2 g, co-cat.: 0.5 wt% Pt, CH_3OH: 50 ml, H_2O: 220 ml, Xe lamp, 300 W, $\lambda > 420$ nm). The rate of H_2 evolution from CH_3OH/H_2O solution in the first 25 h is about 18.1 μmol/h·gcat. for the photocatalyst $BaCo_{1/3}Nb_{2/3}O_3$ prepared by the sol-gel method, much higher than that for the photocatalyst $BaCo_{1/3}Nb_{2/3}O_3$ prepared by the solid state reaction process (about 3.5 μmol/h·gcat.). It means the larger surface area of the photocatalyst powder leads to the production of more H_2. After H_2 evolution from CH_3OH/H_2O solution, the crystal structure of the residue was checked by X-ray diffraction. No any new phase could be found from X-ray diffraction, indicating that $BaCo_{1/3}Nb_{2/3}O_3$ was stable during H_2 evolution reaction. It means that the photocatalytic activity of the photocatalyst $BaCo_{1/3}Nb_{2/3}O_3$ as observed under visible light irradiation should be ascribed to the photocatalytic reaction.

In conclusion, the photocatalyst $BaCo_{1/3}Nb_{2/3}O_3$ has been synthesized by using a sol-gel process. $BaCo_{1/3}Nb_{2/3}O_3$ powder shows a lower crystallizing temperature and the large surface area, as compared with that prepared by a solid state reaction process. The measurement on the photocatalytic activity of $BaCo_{1/3}Nb_{2/3}O_3$ under visible light irradiation($\lambda > 420$ nm) shows that the surface area of the photocatalyst powder plays a very important role in the photocatalytic activity. By increasing the surface area and optimizing the reaction condition, $BaCo_{1/3}Nb_{2/3}O_3$ will become a promising photocatalyst for the production of H_2 by use of solar energy.

References

1. K. HONDA and A. FUJISHIMA, *Nature* **238** (1972) 37.
2. R. ASAHI, T. MORIKAWA, T. OHWAKI, K. AOKI and Y. TAGA, *Science* **293** (2001) 269.
3. Z. ZOU, J. YE, K. SAYAMA and H. ARAKAWA, *Nature(Lond.)* **414** (2001) 625.
4. K. DOMEN, A. KUDO and T. ONISHI, *J. Catal.* **102** (1986) 92.
5. A. KUDO, H. KADO and S. NAKAGAWA, *J. Phys. Chem. B* **104** (2000) 571.
6. J. XU and M. GREENBLATT, *J. Solid State Chem.* **121** (1996) 273.
7. D. E. SCAIFE, *Sol. Energy* **25** (1980) 41.
8. A. L. LINSEBIGLER, G. LU and J. T. YATES JR, *Chem. Rev.* **95** (1995) 735.
9. A. KUDO, H. KATO and S. NAKAGAWA, *J. Phys. Chem. B* **104** (2000) 571.

10. J. YIN, Z. ZOU and J. YE, *J. Phys. Chem. B* **107** (2003) 4936.
11. M. D. FONTANA, G. METRAT, J. L. SERVOIN and F. GERVAIS, *J. Phys. C: Solid State Phys.* **16** (1984) 483.
12. A. SCALABRIN, A. S. CHAVES, D. S. SHIM and S. P. S. PORTO, *Phys. Stat. Sol. (b)* **79** (1977) 731.
13. A. G. SOUZA FILHO, K. C. V. LIMA, A. P. AYALA, I. GUEDES, P. T. C. FREIRE, F. E. A. MELO, J. MENDES FILHO, E. B. ARAUJO and J. A. EIRAS, *Phys. Rev. B* **66** (2002) 132107.
14. C. H. PERRY and B. N. KHANNA, *Phys. Rev.* **135** (1964) A408.
15. F. GALASSO, L. KATZ and R. WARD, *J. Am. Chem. Soc.* **81** (1959) 820.
16. F. GALASSO and W. DARBY, *J. Phys. Chem.* **66** (1962) 131.

Received 25 May 2004
and accepted 25 May 2005